

# Climate-simulated raceway pond culturing: quantifying the maximum achievable annual biomass productivity of *Chlorella sorokiniana* in the contiguous USA

M. Huesemann<sup>1</sup> · A. Chavis<sup>1</sup> · S. Edmundson<sup>1</sup> · D. Rye<sup>1</sup> · S. Hobbs<sup>1</sup> · N. Sun<sup>2</sup> · M. Wigmosta<sup>2</sup>

Received: 3 March 2017 / Revised and accepted: 28 August 2017 / Published online: 13 September 2017  
© Springer Science+Business Media B.V. 2017

**Abstract** *Chlorella sorokiniana* (DOE 1412) emerged as one of the most promising microalgae strains from the NAABB consortium project and was found to have a remarkable doubling time under optimal conditions of 2.57 h<sup>-1</sup>. However, its maximum achievable annual biomass productivity in outdoor ponds in the contiguous USA has not yet been demonstrated. In order to address this knowledge gap, this alga was cultured in indoor LED-lighted and temperature-controlled raceways in nutrient replete freshwater (BG-11) medium at pH 7 under conditions simulating the daily sunlight intensity and water temperature fluctuations during three seasons in Southern Florida, an optimal outdoor pond culture location for this organism identified by prior biomass growth modeling. Prior strain characterization indicated that the average maximum specific growth rate ( $\mu_{\max}$ ) at 36 °C declined continuously with pH, with  $\mu_{\max}$  corresponding to 5.92, 5.83, 4.89, and 4.21 day<sup>-1</sup> at pH 6, 7, 8, and 9, respectively. In addition, the maximum specific growth rate declined nearly linearly with increasing salinity until no growth was observed above 35 g L<sup>-1</sup> NaCl. In the climate-simulated culturing studies, the volumetric ash-free dry weight-based biomass productivities during the linear growth phase were 57, 69, and 97 mg L<sup>-1</sup> day<sup>-1</sup> for 30-year averaged light and temperature

simulations for January (winter), March (spring), and July (summer), respectively, which correspond to average areal productivities of 11.6, 14.1, and 19.9 g m<sup>-2</sup> day<sup>-1</sup>. The photosynthetic efficiencies (PAR) in these three climate-simulated pond culturing experiments ranged from 4.1 to 5.1%. The annual biomass productivity was estimated as ca. 15 g m<sup>-2</sup> day<sup>-1</sup>, nearly double the US Department of Energy (DOE) 2015 State of Technology annual cultivation productivity of 8.5 g m<sup>-2</sup> day<sup>-1</sup>, but still well below the projected DOE 2022 target of ca. 25 g m<sup>-2</sup> day<sup>-1</sup> required for economic microalgal biofuel production, indicating the need for additional research.

**Keywords** *Chlorella sorokiniana* · Annual biomass productivity · Climate-simulation pond culture · Maximum specific growth rate as a function of pH · Maximum specific growth rate as a function of salinity · Photosynthetic efficiency

## Introduction

In an effort to improve the long-term sustainability of industrial societies dependent on transportation fuels, considerable research is being conducted to replace nonrenewable, petroleum-based fuels with renewable biofuels, including fuels derived from the conversion of microalgae biomass (US DOE 2010). A key challenge in the development of an economically viable microalgae biofuels production process is the identification of strains that exhibit annual biomass productivities of at least 25 g m<sup>-2</sup> day<sup>-1</sup> (US Department of Energy target by 2022) in outdoor culture systems (US DOE, 2012).

As early as 1959, *Chlorella* spp. were recognized as very fast-growing microalgae (Sorokin 1959) and have since been commercially produced for human and animal nutrition

**Electronic supplementary material** The online version of this article (<https://doi.org/10.1007/s10811-017-1256-6>) contains supplementary material, which is available to authorized users.

✉ M. Huesemann  
michael.huesemann@pnnl.gov

<sup>1</sup> Marine Sciences Laboratory, Pacific Northwest National Laboratory, Sequim, WA 98382, USA

<sup>2</sup> Hydrology Group, Pacific Northwest National Laboratory, Richland, WA 99352, USA

(Spolaore et al. 2006; Kotrbacek et al. 2015). In the recent Department of Energy National Alliance for Advanced Biofuels and Bioproducts (NAABB) consortium research project, *Chlorella sorokiniana* (DOE 1412) was identified as one of the fastest growing and most productive strains among the many that were screened (Neofotis et al. 2016; Lammers et al. 2017; Unkefer et al. 2017). However, despite its promising characteristics, it was not known whether this strain, when cultured in outdoor raceway ponds in the contiguous USA, can achieve the challenging annual biomass productivity targets required to ensure the economic viability of microalgae biofuels.

The objective of this study was to quantify the biomass productivity of *C. sorokiniana* (DOE 1412) in the state-of-the-art PNNL (Pacific Northwest National Laboratory) indoor LED-lighted and temperature-controlled raceway ponds (Huesemann et al. 2017) under nutrient replete and optimal pH and salinity conditions simulating three seasons (winter, spring, and summer) in Southern Florida, which is the geographic region (in the contiguous USA) expected to result in the highest annual biomass productivity, based on detailed strain characterization and predictions by the PNNL Biomass Assessment Tool (Wigmosta et al. 2011) and biomass growth model (Huesemann et al. 2016).

## Materials and methods

**Microorganism and medium** *Chlorella sorokiniana* strain (DOE 1412) was isolated by Dr. Juergen Polle at Brooklyn College, New York (USA) (Neofotis et al. 2016), and grown at pH 7 in freshwater BG-11 medium containing 17.6 mM NO<sub>3</sub> and 0.66 mM PO<sub>4</sub> as described by Huesemann et al. (2013). The high concentration of N and P and periodic monitoring ensured that no cultures were ever nutrient limited during the experiments.

**Measurement of biomass, nitrogen, and phosphate concentrations** The biomass concentration was measured as optical density at 750 nm (OD<sub>750</sub>) and as ash-free dry weight (AFDW, mg L<sup>-1</sup>), as described in Van Wagenen et al. (2012). The concentrations of nitrogen and orthophosphate in the culture supernatant were determined colorimetrically (i.e., EMD Chemicals 10020-1 and Hach Aquacheck 2757150 for nitrogen and Orbeco Hellige L147250 for phosphate) to ensure that soluble nitrogen and phosphorus were available in the culture medium during the entire experiment.

**Quantification of the biomass light absorption coefficient ( $k_a$ )** The biomass light absorption coefficient  $k_a$  was determined for dilute culture samples (OD<sub>750</sub> < 0.3) in a 1-cm path-length cuvette by measuring light absorption relative to a medium blank with a LI-COR quantum sensor (PAR, LI-190) and calculated using the Beer-Lambert law as described

in Huesemann et al. (2013). Lighting was provided by a multi-colored LED panel simulating sunlight intensity and PAR spectrum (Fig. S1).

**Measurement of the maximum specific growth rate ( $\mu$ ) as a function of pH** The maximum specific (exponential) growth rate of *C. sorokiniana* (DOE 1412) was measured in Phenometrics photobioreactor (ePBR™, Lucker et al. 2014) cultures at 36 °C, the optimum growth temperature for this strain (Huesemann et al. 2016), at four different pH set points, i.e., 6, 7, 8, and 9. The pH was feedback-controlled via on-demand addition of pure CO<sub>2</sub> in 1 s pulses. All cultures were continuously sparged with air to remove photosynthetically produced oxygen, a potential growth inhibitor, and to provide vigorous mixing in addition to magnetic stirring at 400 rpm. The cultures were maintained at a constant depth of 15 cm, equivalent to a volume of 335 mL. Lighting was provided continuously by a white LED at an intensity of 1000  $\mu\text{mol photons m}^{-2} \text{s}^{-1}$  at the culture surface. Following inoculation, the cultures were allowed to grow exponentially until reaching an OD<sub>750</sub> of 0.12, which ensured, according to Beer-Lambert's law using experimentally determined light absorption (extinction) coefficients ( $k_a$ ), that all cells in the 15 cm deep culture received above saturating light intensity (> 250  $\mu\text{mol photons m}^{-2} \text{s}^{-1}$ ), i.e., there was no light limitation. Samples for OD<sub>750</sub> measurement were taken every few hours from each ePBR™ during the daily repeated exponential growth experiments. The maximum specific growth rate ( $\mu$ ) at each pH set point was determined from the ln(OD<sub>750</sub>) versus time slope.

**Measurement of the maximum specific growth rate ( $\mu$ ) as a function of salinity** The maximum specific (exponential) growth rate of *C. sorokiniana* (DOE 1412) was measured repeatedly in dilute shaker flask cultures (100 mL) at room temperature (ca. 23 °C) at eight salinities, i.e., 0, 0.5, 1, 2.5, 5, 10, 20, and 40 g L<sup>-1</sup> NaCl. The pH was maintained at 7 via continuous sparging with CO<sub>2</sub>-enriched air (0.5% CO<sub>2</sub>). Lighting was provided continuously by overhead fluorescent lights providing ca. 500  $\mu\text{mol photons m}^{-2} \text{s}^{-1}$  at the top of the flasks. Following inoculation, the cultures were allowed to grow exponentially until reaching an OD<sub>750</sub> of 0.3, which ensured that all cells in the 4 cm deep shaker flask culture received above saturating light intensity (> 250  $\mu\text{mol photons m}^{-2} \text{s}^{-1}$ ), i.e., there was no light limitation (Huesemann et al. 2016). Samples for OD<sub>750</sub> measurement were taken every few hours from each flask culture, and the maximum specific growth rate ( $\mu$ ) at each salinity was determined from the ln(OD<sub>750</sub>) versus time slope.

**Indoor climate-simulation raceway pond culture experiments** Two indoor LED-lighted and temperature-controlled raceway ponds, as described in Huesemann et al. (2017) and as shown in Fig. S1, were used to culture *C. sorokiniana* (DOE

1412) under climate-simulated conditions. As demonstrated earlier, when these indoor pond cultures are operated using the same light intensity and water temperature scripts as measured in outdoor ponds, both biomass growth and productivity are similar in the climate-simulation and outdoor raceways (Huesemann et al. 2017). The ponds were operated in batch culture mode at pH 7 via periodic feedback-controlled CO<sub>2</sub> sparging and at a constant depth of 20.5 cm, equivalent to a total culture volume of ca. 660 L. In previous experiments (Edmundson and Huesemann 2015; Huesemann et al. 2016), we extensively characterized *C. sorokiniana* (DOE 1412) by measuring the light extinction coefficient ( $k_d$ ), the rate of biomass loss in the dark as a function of temperature and light intensity preceding the dark period, and the maximum specific growth rate as a function of light intensity and temperature. In this study, we entered these strain-specific parameters into the enhanced biomass growth model (Huesemann et al. 2016) that is coupled with the Biomass Assessment Tool (BAT, Perkins and Richmond, 2004; Wigmosta et al. 2011) to identify outdoor pond locations of maximum annual biomass productivity. After identifying the best outdoor pond location in the contiguous USA as Key West, Florida (see Fig. S2), the BAT used 30-year meteorological data to generate light intensity and water temperature scripts for use in this study. The replicate indoor climate-simulation ponds were operated using light and temperature scripts for the months of January (winter), March (spring), and July (summer) (Figs. 1 and S3). It should be noted that while the Key West, Florida, location is best for achieving the optimum annual biomass productivity for this strain, it is not practical for large-scale microalgae biomass production given severe land limitations.

**Calculation of photosynthetic efficiencies** For a given cultivation time period, photosynthetic efficiency (PE) is the ratio of energy captured by biomass divided by the light (PAR) energy absorbed by the culture. The caloric energy content of *Chlorella* biomass was assumed to be 24.7 kJ g<sup>-1</sup> AFDW (Williams and Laurens 2010), which is higher than the commonly used value of 22 kJ g<sup>-1</sup> (Morita et al. 2000) due to the absence of ash (Change to Bechet et al. 2013). The light energy absorbed by the culture during the linear growth phase (AFDW > 200 mg L<sup>-1</sup>) was obtained by integration of all light intensity “script” values (see Figs. 1 and S3 for examples), assuming that 1 W m<sup>-2</sup> (PAR) = 4.94 μmol photons m<sup>-2</sup> s<sup>-1</sup> (Doucha and Livansky 2006, 2009).

## Results and discussion

### Effects of pH on the maximum specific growth rate

The average maximum specific growth rate at 36 °C declined continuously with increasing pH, with  $\mu_{\max}$  ( $\pm$  std error,  $n = 6$ )

corresponding to 5.92 ( $\pm$  0.14), 5.83 ( $\pm$  0.14), 4.89 ( $\pm$  0.21), and 4.21 ( $\pm$  0.16) day<sup>-1</sup> at pH 6, 7, 8, and 9, respectively. In order to compare these data with findings from other studies involving *Chlorella* species, the relative growth rate, normalized to the rate at pH 7 (= 100%), was plotted as a function of pH (Fig. 2). Our results confirm the earlier observations by Morita et al. (2000) that the specific growth rate of *C. sorokiniana* is slightly higher at pH 6 than at pH 7. The specific growth rate declines substantially with decreasing pH, but *C. sorokiniana* is still capable of significant growth at pH 3. In summary, *C. sorokiniana* is tolerant to large fluctuations in pH (i.e., at least from pH 3 to pH 9) without detrimental impact on growth, and the maximum specific growth rate is highest at pH 6.

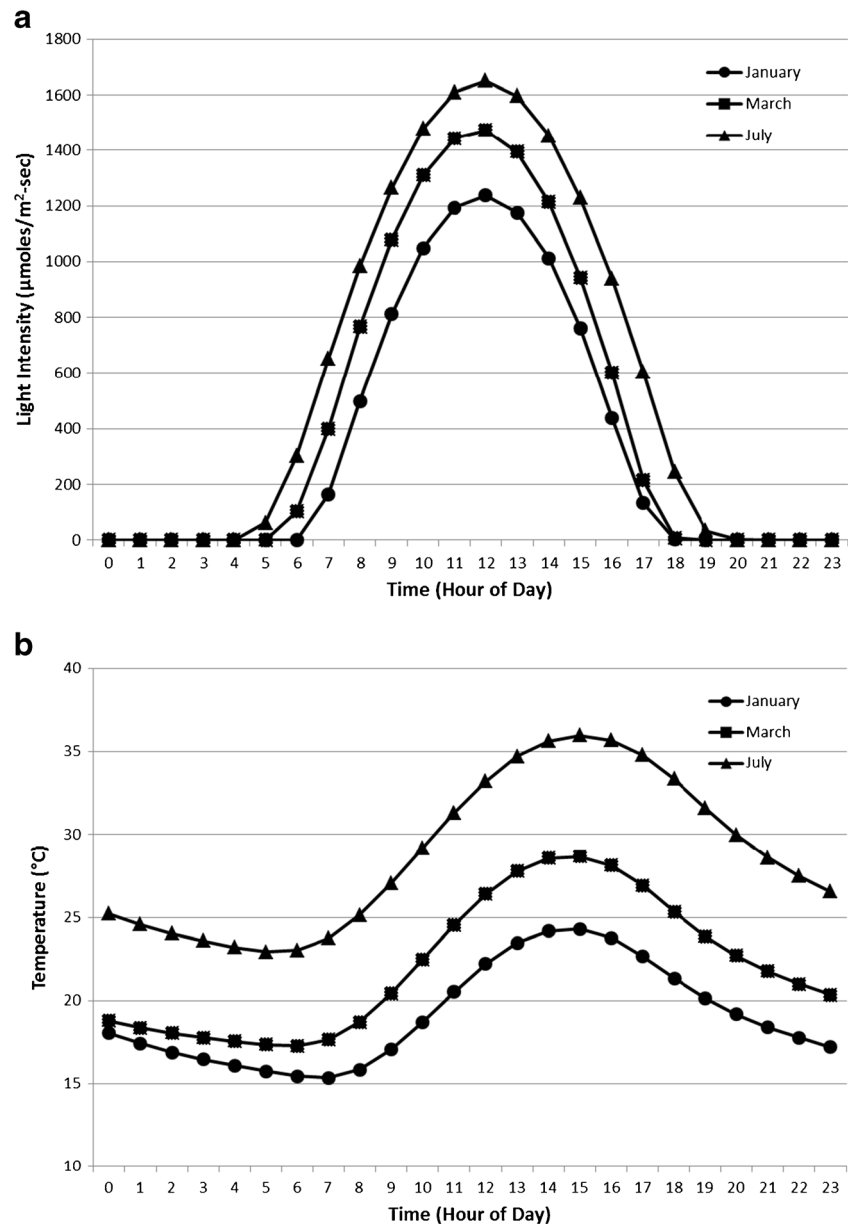
Since no other growth rate versus pH data could be found in the published literature for the species used in this study (i.e., *C. sorokiniana*), the phototrophic growth versus pH behavior of a related species, *Chlorella vulgaris*, is shown in Fig. 2 for comparison. While *C. vulgaris* also exhibits growth over a wide range of pH values, optimum growth is observed at pH 7.5 rather than pH 6, as for *C. sorokiniana*. Similarly, Moheimani (2013) reported the highest biomass and lipid productivity in semi-continuous cultures of *Chlorella* sp. at pH 7.5. Goldman et al. (1982) observed a gradual decline in steady-state biomass concentration and productivity of continuous cultures of *C. vulgaris* as the pH was increased from 8 to 10.5, the maximum pH value at which growth was observed. In summary, the growth rate versus pH response differs among different *Chlorella* species. Although the highest specific growth rate of *C. sorokiniana* (DOE1412) was observed at pH 6, the climate-simulation ponds were operated at pH 7 to reduce CO<sub>2</sub> outgassing and improve the CO<sub>2</sub> utilization efficiency.

### Effects of salinity on the maximum specific growth rate

The maximum specific growth rate declined nearly linearly with increasing salinity until minimal or no growth was observed above 35 g L<sup>-1</sup> NaCl (Fig. 3). The NaCl concentration resulting in a 50% reduction in maximum specific growth rate (EC<sub>50</sub>) of *C. sorokiniana* is around 20 g L<sup>-1</sup>. This is in contrast to findings by Convalves et al. (2005) who reported EC<sub>50</sub> values of 5.1 g L<sup>-1</sup> NaCl for *Chlorella vulgaris*, indicating that this species is much more sensitive to salinity stress than *C. sorokiniana*. On the other hand, when evaluating a *C. vulgaris* isolate from Antarctica, Yandu et al. (2010) still observed significant growth, although much reduced relative to the freshwater control, at 30 g L<sup>-1</sup> NaCl.

The salinity tolerances of freshwater *Chlorella* spp. are understandably much less than in strains isolated from seawater (Batterton and Baalen 1971; Fabregas et al. 1984; Renaud and Parry 1994; Sogaard et al. 2011) or hypersaline environments (Van Auken and McNulty 1973) but are

**Fig. 1** Incident solar radiation (a) and pond water temperature (b) predicted by the Biomass Assessment Tool for 20.5 cm deep ponds in Key West, Florida, during the first day of January (winter), March (spring), and July (summer). Light and temperature scripts for each respective entire month were used for the climate-simulated culturing of *Chlorella sorokiniana* (DOE 1412), see Fig. S3 as an example for the month of July



comparable to other freshwater microalga such as *Scenedesmus obliquus*, whose growth was significantly reduced relative to the freshwater control at 0.3 M ( $17.4 \text{ g L}^{-1}$ ) NaCl (Kaewkannetra et al. 2012). The observation, as shown in Fig. 3, that the maximum specific growth rate of *C. sorokiniana* is only marginally reduced at  $5 \text{ g L}^{-1}$  NaCl relative to the zero salinity control suggests, based on our Huesemann et al. (2016) biomass growth model predictions where maximum specific growth rate is positively related to productivity, that this strain could be cultured in brackish water (< 3% salinity) with minimum negative impact on biomass productivity. Nevertheless, the climate-simulation pond culture experiments in this study were conducted with freshwater BG-11 medium to determine the maximum achievable

biomass productivity under the given light and temperature regimes.

#### Biomass productivities and photosynthetic efficiencies in climate-simulation pond cultures

Duplicate indoor climate-simulation pond culture experiments were conducted using 30-year average light and temperature scripts for January, March, and July, i.e., months representative of the winter, spring, and summer seasons in Southern Florida (Fig. 1). During these experiments, the LED lighting and temperature control system functioned virtually flawlessly, as indicated by the similarity between set point and measured light intensity and water temperature values at all

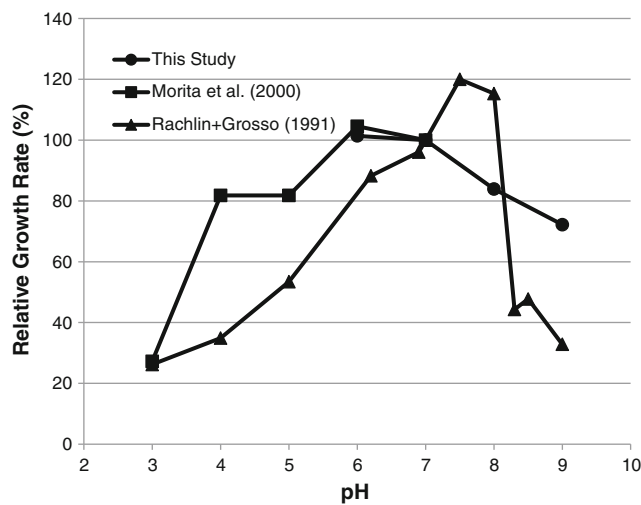


**Fig. 2** Relative growth rate, normalized to the growth rate at pH 7, of *Chlorella sorokiniana* (Morita et al. 2000; this study) and *Chlorella vulgaris* (Rachlin and Grosso 1991) as a function of culture pH

consecutive time points (Fig. S3). As expected, there was a significant seasonal difference in the monthly average daytime/nighttime water temperatures, i.e., 20.7/17.5 °C, 24.5/19.9 °C, and 29.9/25.4 °C, and in the monthly maximum/minimum water temperatures, i.e., 26.3/14.5 °C, 30.8/16.8 °C, and 36/22.4 °C, for January, March, and July, respectively (Table 1).

By contrast, while the average daytime incident photosynthetically active radiation was lowest in January (664 μmol photons m<sup>-2</sup> s<sup>-1</sup>), it was surprisingly similar for March (845 μmol photons m<sup>-2</sup> s<sup>-1</sup>) and July (843 μmol photons m<sup>-2</sup> s<sup>-1</sup>) (Table 1). A likely explanation is that while the peak (noon) solar irradiance is higher and the day length longer in July than in March, the increased humidity, cloudiness, and incidence of thunderstorms in July reduce

the average daily PAR to the same level as observed in spring (March), the dry season in Florida.

As shown in Fig. 4, the biomass concentration, measured as optical density (OD<sub>750</sub>), increased fastest with time in the July climate-simulation pond culture, leveling off to about 6.5 at the end of the experiment. The rate of OD<sub>750</sub> increase was comparatively much slower in the January and March simulation ponds but both of these cultures exhibited similar growth behavior despite the fact that the January culture received much less incident light and was subjected to lower average daytime temperatures than the March culture (Fig. 4 and Table 1). Since OD<sub>750</sub> measurements are based on light scattering, which is affected by cell size and number, and to some degree on light absorption which is influenced by cellular pigment content and composition, optical density is a less reliable indicator of biomass concentration than ash-free dry weight (AFDW) (Edmundson and Huesemann 2015).

Indeed, when AFDW was plotted as a function of time for the three season climate-simulation pond cultures, the rate of biomass growth was highest for July, second highest for March, and lowest for January (Fig. 5). Since the average daytime PAR was about the same in July and March, the much higher linear-phase biomass productivity in July was due to the 5.4 °C (29.9 vs. 24.5 °C) higher daytime average water temperature (Table 1 and Fig. 1 in Huesemann et al. 2016). The linear-phase biomass productivity in March was higher than in January as a result of both higher average daytime PAR (845 vs. 664 μmol photons m<sup>-2</sup> s<sup>-1</sup>) and higher daytime water temperature (24.5 vs. 20.7 °C). The July cultures reached a final AFDW of about 1400 mg L<sup>-1</sup>, while the final AFDW was slightly below 1000 mg L<sup>-1</sup> in the January and March cultures. The difference in growth kinetics, depending on whether OD<sub>750</sub> or AFDW is used as a measure of biomass concentration, is also reflected in different AFDW-OD<sub>750</sub> correlations for the three climate-simulation experiments.

**Fig. 3** Maximum specific growth rate of *Chlorella sorokiniana* (DOE 1412) at 27 °C as a function of NaCl concentration. Errors bars represent one standard deviation (*n* = 4 for 0, 5, 10, and 15 g L<sup>-1</sup> NaCl; *n* = 3 for 12.5, 17.5, and 20 g L<sup>-1</sup> NaCl; *n* = 2 for 25 and 30 g L<sup>-1</sup> NaCl; and *n* = 1 for 35 and 40 g L<sup>-1</sup> NaCl)

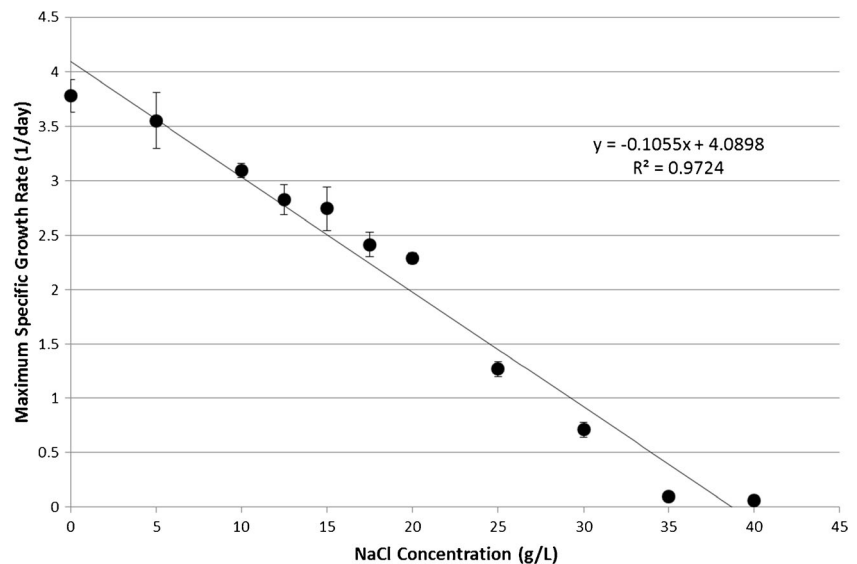




**Table 1** Areal biomass productivity and photosynthetic efficiency (PAR) of different *Chlorella* spp. grown under different conditions in indoor or outdoor cultivation systems

Culture system	Culture conditions	Areal productivity	Photosynthetic efficiency (PAR)
Indoor climate-simulation ponds (this study)	Species: <i>Chlorella sorokiniana</i> Culture depth: 20.5 cm pH: 7.5 Avg. daytime PAR: 664 $\mu\text{mol photons m}^{-2} \text{ s}^{-1}$ Avg. daytime culture temperature: 20.7 $\pm$ 3.5 °C (stdev) Avg. nighttime culture temperature: 17.5 $\pm$ 1.7 °C (stdev) Simulated month: January	Linear phase: 11.6 $\text{g m}^{-2} \text{ day}^{-1}$ Min instantaneous: 7.1 $\text{g m}^{-2} \text{ day}^{-1}$ Max instantaneous: 17.1 $\text{g m}^{-2} \text{ day}^{-1}$	4.82%
Indoor climate-simulation ponds (this study)	Species: <i>Chlorella sorokiniana</i> Culture depth: 20.5 cm pH: 7.5 Avg. daytime PAR: 845 $\mu\text{mol photons m}^{-2} \text{ s}^{-1}$ Avg. daytime culture temperature: 24.5 $\pm$ 4.0 °C (stdev) Avg. nighttime culture temperature: 19.9 $\pm$ 1.7 °C (stdev) Simulated month: March	Linear phase: 14.1 $\text{g m}^{-2} \text{ day}^{-1}$ Min instantaneous: 8.7 $\text{g m}^{-2} \text{ day}^{-1}$ Max instantaneous: 19.0 $\text{g m}^{-2} \text{ day}^{-1}$	4.11%
Indoor climate-simulation ponds (this study)	Species: <i>Chlorella sorokiniana</i> Culture depth: 20.5 cm pH: 7.5 Avg. daytime PAR: 843 $\mu\text{mol photons m}^{-2} \text{ s}^{-1}$ Avg. daytime culture temperature: 29.9 $\pm$ 4.3 °C (stdev) Avg. nighttime culture temperature: 25.4 $\pm$ 1.7 °C (stdev) Simulated Month: July	Linear phase: 19.9 $\text{g m}^{-2} \text{ day}^{-1}$ Min instantaneous: 7.6 $\text{g m}^{-2} \text{ day}^{-1}$ Max instantaneous: 36.1 $\text{g m}^{-2} \text{ day}^{-1}$	5.13%
Raceway ponds in greenhouse (Hase et al. 2000)	Species: marine and freshwater <i>Chlorella</i> sp. Culture depth: 26 cm pH: 5.7–6.4 PAR: 2.5–7.8 $\text{MJ m}^{-2} \text{ day}^{-1}$ Culture temperature: 19.7–26 °C Culture mode: semi-continuous Location: Sendai City, Japan Months: June–October	13.2 (7–21) $\text{g m}^{-2} \text{ day}^{-1}$	4.9–8.1%
Conical helical tubular photobioreactors (Morita et al. 2000)	Species: <i>Chlorella sorokiniana</i> Culture depth: NA pH: 5.2–6.5 (10% CO <sub>2</sub> in air) PAR: 484 $\mu\text{mol photons m}^{-2} \text{ s}^{-1}$ (12-h light/12-h dark cycle) Culture temperature: 42 °C Culture mode: batch Location: indoors, Japan	34.4 $\text{g m}^{-2} \text{ day}^{-1}$	8.67%
Outdoor open thin-layer photobioreactor (Doucha and Livansky 2006)	Species: <i>Chlorella</i> sp. Culture depth: 0.6 cm pH: 7.9–8.35 PAR: 140–250 $\text{W m}^{-2}$ (692–1235 $\mu\text{mol photons m}^{-2} \text{ s}^{-1}$ ) Culture temperature: 29.5 $\pm$ 6 (stdev) °C Culture mode: batch Location: Trebon, Czech Republic (49° N) Month: July	23.5 $\text{g m}^{-2} \text{ day}^{-1}$	6.48%
Outdoor open thin-layer photobioreactor (Doucha and Livansky 2006)	Species: <i>Chlorella</i> sp. Culture depth: 0.6 cm	11.1 $\text{g m}^{-2} \text{ day}^{-1}$	5.98%

**Table 1** (continued)

Culture system	Culture conditions	Areal productivity	Photosynthetic efficiency (PAR)
Outdoor open thin-layer photobioreactor (Doucha and Livansky 2006)	pH: 7.9–8.35 (assumed to be similar as in July) PAR: 50–175 W m <sup>-2</sup> (247–864 μmol photons m <sup>-2</sup> s <sup>-1</sup> ) Culture temperature: 13–23 °C (daily avg. low/high) Culture mode: batch Location: Trebon, Czech Republic (49° N) Month: September Species: <i>Chlorella</i> sp. Culture depth: 0.8 cm	32.2 g m <sup>-2</sup> day <sup>-1</sup>	5.42%
Outdoor open thin-layer photobioreactor (Doucha and Livansky 2006)	pH: 7.4–8.0 PAR: 50–450 W m <sup>-2</sup> (247–2223 μmol photons m <sup>-2</sup> s <sup>-1</sup> ) Culture temperature: 33.5 ± 2 (stdev) °C Culture mode: batch Location: Kalamata, Greece (37° N) Month: July Species: <i>Chlorella</i> sp. Culture depth: 0.8 cm	18.1 g m <sup>-2</sup> day <sup>-1</sup>	6.07%
Outdoor open thin-layer photobioreactor (Doucha and Livansky 2006)	pH: 7.4–8.0 (assumed to be similar as in July) PAR: 50–250 W m <sup>-2</sup> (247–1235 μmol photons m <sup>-2</sup> s <sup>-1</sup> ) Culture temperature: 27.1 ± 4.1 (stdev) °C Culture mode: batch Location: Kalamata, Greece (37° N) Month: October Species: <i>Chlorella</i> sp. (thermophilic) Culture depth: 0.6–0.7 cm	38.2 g m <sup>-2</sup> day <sup>-1</sup>	9%
Thin panel photobioreactor with continuous LED lighting (Cuaresma et al. 2009)	pH: 7.3–7.8 PAR (avg daily): 125–162 W m <sup>-2</sup> (617–800 μmol photons m <sup>-2</sup> s <sup>-1</sup> ) Culture temperature: 20–38.5 °C Culture mode: fed-batch Location: Trebon, Czech Republic (49° N) Month: July Species: <i>Chlorella sorokiniana</i> Culture depth: 1.4 cm	185 g m <sup>-2</sup> day <sup>-1</sup>	11.71% (1 g mole <sup>-1</sup> photons) <sup>a</sup>
Thin panel photobioreactor with continuous LED lighting (Cuaresma-Franco et al. 2012)	pH: 6.7 LED light intensity at 637 nm: 2100 μmol photons m <sup>-2</sup> s <sup>-1</sup> Culture temperature: 37 ± 1 °C (constant) Culture mode: continuous Location: indoors, The Netherlands Species: <i>Chlorella sorokiniana</i> Culture depth: 1.4 cm	40.3 g m <sup>-2</sup> day <sup>-1</sup>	5.85% (0.5 g mole <sup>-1</sup> photons) <sup>a</sup>
Thin panel photobioreactor with continuous LED lighting (Cuaresma-Franco et al. 2011)	pH: 6.7 LED light intensity at 637 nm: 800 μmol photons m <sup>-2</sup> s <sup>-1</sup> Culture temperature: 20 °C (constant) Culture mode: continuous Location: indoors, The Netherlands Species: <i>Chlorella sorokiniana</i> Culture depth: 1.4 cm	94.1 g m <sup>-2</sup> day <sup>-1</sup>	14.05% (1.2 g mole <sup>-1</sup> photons) <sup>a</sup>

**Table 1** (continued)

Culture system	Culture conditions	Areal productivity	Photosynthetic efficiency (PAR)
Outdoor column photobioreactor (Bechet et al. 2013)	Culture temperature: 38 °C (constant $\mu\text{mol photons m}^{-2} \text{s}^{-1}$ ) Culture mode: continuous Location: indoors, The Netherlands Species: <i>Chlorella sorokiniana</i> PBR dimensions: 2 m height $\times$ 0.19 m internal diameter pH: $6.9 \pm 0.1$ PAR (avg daily): $350 \pm 50$ (95% CI) $\mu\text{mol photons m}^{-2} \text{s}^{-1}$ Culture temperature: $< 41$ °C Culture mode: batch Location: Singapore	$10 \pm 2.2 \text{ g m}^{-2} \text{ day}^{-1}$ (illuminated bioreactor surface area)	$10.2 \pm 1.06\%$ $(4.8 \pm 0.5\%$ (total solar radiation))

<sup>a</sup> Unit conversion based on  $22 \text{ kJ g}^{-1}$  dry weight (Morita et al. 2000) and  $187.9 \text{ kJ mole}^{-1}$  of photons with wavelength of 637 nm, per  $E = h * c/\lambda$ , with  $E$  = energy quantum of photon,  $h$  = Planck constant,  $c$  = speed of light, and  $\lambda$  = wavelength

For January and July,  $\text{AFDW (mg L}^{-1}) = 218 \cdot \text{OD}_{750} + 13.3$  ( $R^2 > 0.99$ ) and  $\text{AFDW (mg L}^{-1}) = 201 \cdot \text{OD}_{750} - 8.5$  ( $R^2 > 0.99$ ), respectively (Fig. S4), correlations that are similar to those observed in numerous previous experiments with *C. sorokiniana* in our laboratory (Huesemann et al. 2013). By contrast,  $\text{AFDW (mg L}^{-1}) = 278 \cdot \text{OD}_{750} + 19.7$  ( $R^2 > 0.99$ ) for the March cultures (Fig. S4). The reasons for this large deviation in AFDW- $\text{OD}_{750}$  correlation in the March pond experiments relative to the January and July cultures are not known. It is possible that the cell size in the March cultures was smaller, resulting in increased light scattering; however, no cell size measurements were taken and thus this hypothesis remains untested. Compared to the January and July pond cultures, which had somewhat similar average biomass light

absorption coefficients  $k_a$  (PAR) over the entire duration of the experiment (i.e.,  $64 \pm 2.5\sigma$  and  $68 \pm 3.5\sigma$ , respectively), the March cultures also had an uncharacteristically high average  $k_a$  value of  $90.2 \pm 6.1\sigma$ . In previous pond culture experiments with *C. sorokiniana*, we observed significant increases in  $k_a$  values upon invasion of the culture by rotifers (data not shown). Thus, increases in  $k_a$  may be an indicator of culture stress, and in this context, it is interesting to note that the March cultures exhibited the lowest photosynthetic efficiency among all experiments (Table 1). Periodic microscopic inspection of pond culture samples confirmed the absence of rotifers or other predators; therefore, the reason for the uncharacteristically high  $k_a$  values in the March cultures remains unknown.

**Fig. 4** Biomass concentration ( $\text{OD}_{750}$ ) as a function of time during batch culture of *Chlorella sorokiniana* (DOE 1412) in PNNL climate-simulation ponds using light and temperature scripts for January, March, and July, as shown in Figs. 1 and S3. Errors bars represent the standard error of the mean,  $n = 2$  ponds

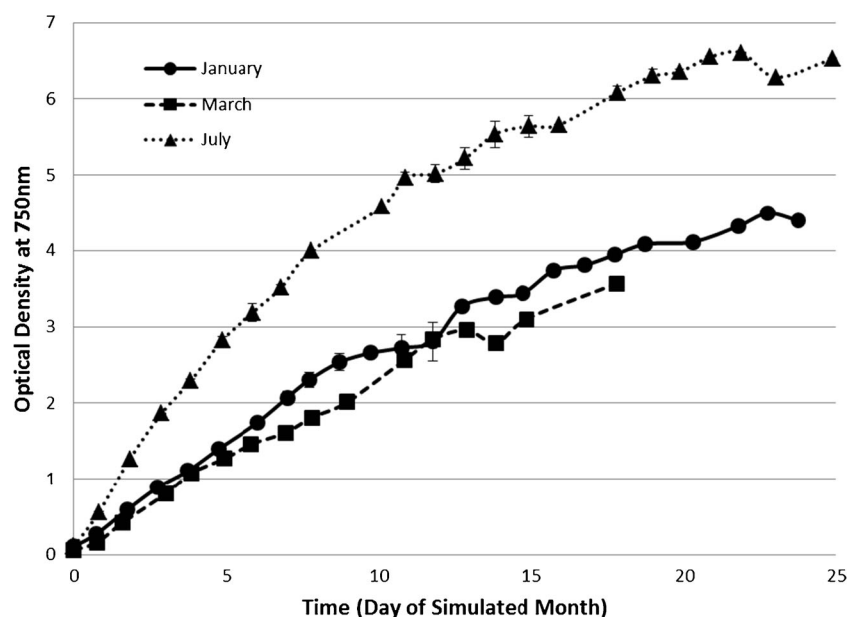
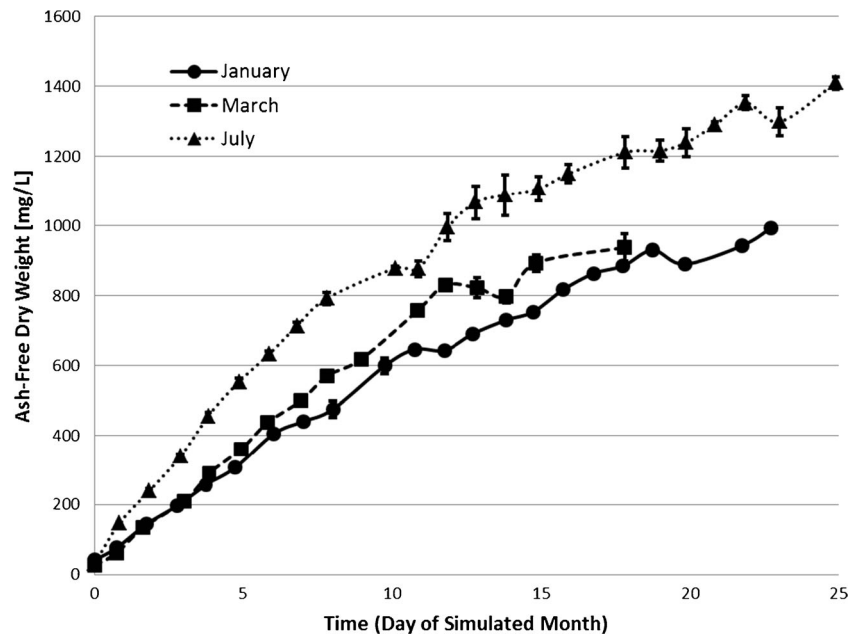




**Fig. 5** Biomass concentration (AFDW) as a function of time during batch culture of *Chlorella sorokiniana* (DOE 1412) in PNNL climate-simulation ponds using light and temperature scripts for January, March, and July, as shown in Figs. 1 and S3. Errors bars represent the standard error of the mean,  $n = 2$  ponds



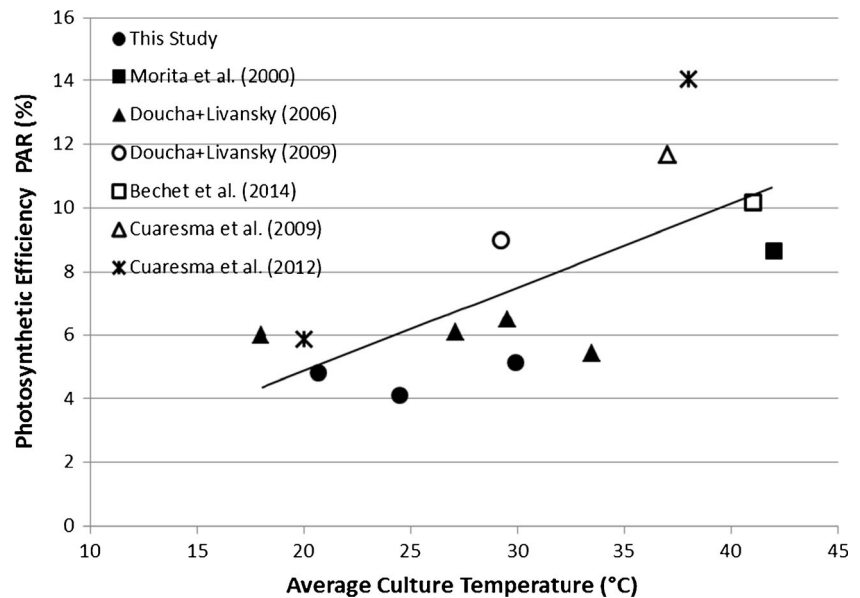
Sustained volumetric biomass productivities were determined for each of the three season climate-simulation experiments from the linear regression slopes (all  $R^2 > 0.99$ ) of average AFDW versus time data during the first 8 to 10 days when linear growth was observed (Fig. S5). The measured volumetric biomass productivities of 57, 69, and 97  $\text{mg L}^{-1} \text{day}^{-1}$  for January, March, and July, respectively, corresponded, for a constant pond culture depth of 20.5 cm, to areal productivities of 11.6, 14.1, and 19.9  $\text{g m}^{-2} \text{day}^{-1}$  (Table 1). It is important to note that the simulated seasons were 30-year average light and temperature data for the Southern Florida location, which moderates both high and low productivity years. This moderation gives a realistic prediction of yields over industrially relevant time scales, but it does not consider extreme weather events such as tropical storms that could severely reduce productivity.

A close inspection of the AFDW versus time data shown in Figs. 5 and S5 reveals that there was a slight variation in slopes between subsequent data points, indicating that volumetric or areal productivities varied during the 10-day linear growth phase. While such variation in “instantaneous” (as opposed to the 10-day linear regression) productivities may be due to analytical variabilities in the AFDW measurements, it may also reflect changes in the growth performance of the cultures, possibly in response to changes in light and temperature (per script programming) or due to unknown physiological causes. The maximum “instantaneous” productivities ( $\pm \sigma, n = 6$ ) for the January, March, and July simulations were  $17.1 \pm 1.1$ ,  $19.0 \pm 0.8$ , and  $36.1 \pm 2.1$  (Table 1). By contrast, the minimum “instantaneous” productivities ( $\pm \sigma, n = 6$ ) for the January, March, and July simulations were  $7.1 \pm 3.1$ ,

$8.7 \pm 2.9$ , and  $7.6 \pm 1.62$  (Table 1). The maximum observed productivities for the July simulation ( $36.1 \text{ g m}^{-2} \text{day}^{-1}$ ) was nearly twice the 10-day linear productivity ( $19.9 \text{ g m}^{-2} \text{day}^{-1}$ ) and is similar to other reported areal productivities of *C. sorokiniana* in thin-layer outdoor ponds (Table 1). Although it is unclear why these high “instantaneous” productivities were not sustained, maximum biomass productivities for the summer run were repeatedly observed in the morning before noon.

Assuming that the areal biomass productivity for the fall season is approximately the same as was measured in March (i.e.,  $14.1 \text{ g m}^{-2} \text{day}^{-1}$ ), the annual sustained biomass productivity was calculated as the average of the four season biomass productivities as ca. 15 ( $14.95 \text{ g m}^{-2} \text{day}^{-1}$ ). The assumption of similar spring and fall biomass productivities is based on the predicted light intensity and water temperature script data which indicate that while the average daily water temperature is about 3 °C lower during the first day of spring than during the first day of fall (i.e., 23.8 vs. 26.9 °C), the maximum daily light intensity is significantly higher during the first day of spring than the first day of fall (i.e., 1577 vs. 1415  $\mu\text{mol photons m}^{-2} \text{s}^{-1}$ ). Since per model predictions for *C. sorokiniana* (DOE 1412), biomass productivity increases with increasing temperature and light intensity (Huesemann et al. 2016), it is assumed that the biomass productivity in spring (lower temperature/higher light intensity) is about the same as in fall (higher temperature, lower light intensity). While the observed productivity of  $15 \text{ g m}^{-2} \text{day}^{-1}$  is nearly double the US Department of Energy 2015 State of Technology annual cultivation productivity of  $8.5 \text{ g m}^{-2} \text{day}^{-1}$ , it is still well below the projected 2022 target of ca.  $25 \text{ g m}^{-2} \text{day}^{-1}$  (US DOE 2016).

**Fig. 6** Photosynthetic efficiency (PAR) of *Chlorella* sp. as a function of average culture temperature for the cultivation studies shown in Table 1. According to the linear least-squares regression,  $PE = 0.26 \cdot T = 0.41$ ,  $R^2 = 0.49$



Since Key West, Florida, was determined via predictions by the PNNL Biomass Assessment Tool (BAT, see above) to be the optimum cultivation location for *C. sorokiniana*, the maximum achievable annual biomass productivity for this strain in standard raceway outdoor pond cultures (20–30 cm depth) is unlikely to exceed  $15 \text{ g m}^{-2} \text{ day}^{-1}$  in the contiguous USA. It may be possible to slightly increase the biomass productivity by varying the pond culture depth for better thermal management. For example, operating ponds at shallower depth during the cold season will increase the daytime water temperatures by a few degrees centigrade and thus slightly increase the daily biomass productivity.

While the medium nitrate concentrations predictably decreased as a function of time in all climate-simulation pond cultures, they never declined below  $500 \text{ mg L}^{-1}$ , confirming nitrogen-replete conditions throughout the experiments (Fig. S6-A). The rate of phosphate uptake from the medium correlated with the volumetric biomass productivities, i.e., the highest rate of phosphate concentration decline with time was observed for July, the next highest for March, and the lowest for January (Fig. S6-B). The final medium phosphate concentrations in the January and March simulation pond cultures were ca.  $30$  and  $20 \text{ mg L}^{-1}$ , confirming phosphate-replete conditions for the duration of the experiments (Fig. S6-B). By contrast, the average phosphate concentration reached nearly non-detectable levels ( $1.5 \text{ mg L}^{-1}$ ) around day 18 in the July simulation ponds. At that time, ca.  $30 \text{ mg L}^{-1}$  phosphate was added to both cultures to ensure phosphate-replete conditions for the remainder of the experiment (Fig. S6-B).

The daily increase and decrease in the concentration of photosynthetically produced dissolved oxygen in the climate-simulation pond cultures mirrored closely the time course of incident solar radiation shown in Fig. 1a, i.e., an increase in

the morning and a decrease in the afternoon, with the maximum concentrations observed around noon (Fig. S7-A). While the dissolved oxygen concentrations in the March and July cultures had a comparatively similar range, i.e., from 6–7 to 26–27  $\text{mg L}^{-1}$ , they ranged from ca. 11 to 36  $\text{mg L}^{-1}$  in the January simulation ponds. Much of the observed differences in dissolved oxygen concentrations among the three climate-simulation ponds can be explained by the decline in solubility of oxygen with increasing pond water temperatures (e.g., 9.1, 8.3, and 7.6  $\text{mg L}^{-1}$  at 20, 25, and 30 °C, respectively). All ponds reached supersaturated dissolved oxygen concentrations, i.e., 300% over the corresponding oxygen solubility at the respective temperatures. As the algae produce oxygen via photosynthesis, warmer water temperatures cause faster escape of oxygen gas from solution due to lower solubility, especially in well-mixed raceway ponds. It is interesting to note that the dissolved oxygen concentration in the March climate simulation was lower than would be expected based on observations in the other two climate simulations, which may be another indication, in addition to the uncharacteristically high biomass light absorption coefficient  $k_a$  and lower photosynthetic efficiency that was observed in the March simulation ponds (see above), that growth was suboptimal for unknown reasons.

The amplitude of the diurnal variations in dissolved oxygen concentrations (i.e., the difference between the highest and lowest daily DO concentration) declined with time as the culture increased in density. For example, in the July climate-simulation cultures, the amplitude in DO concentration at the beginning of the experiment was about  $20 \text{ mg L}^{-1}$  ( $26 \text{ mg L}^{-1}$  at noon,  $6 \text{ mg L}^{-1}$  at night) while it was only about  $9 \text{ mg L}^{-1}$  ( $13 \text{ mg L}^{-1}$  at noon,  $4 \text{ mg L}^{-1}$  at night) at day 24 of the experiment (Fig. S7-B). The declining amplitudes of daily DO concentration swings is most likely caused by a combination of a slowdown in biomass productivity with time and a

decline in the average light intensity below the saturating light intensity (e.g., ca. 250  $\mu\text{mol photons m}^{-2} \text{s}^{-1}$ , see Huesemann et al. 2016), that latter of which occurs within the first few days of the experiment based on light attenuation measurements (data not shown).

The dissolved oxygen concentrations observed in this study are comparable to those reported by Doucha and Livansky (2006) for *Chlorella* sp. cultured in outdoor open thin-layer photobioreactors, where DO levels ranged from ca. 23 to 36  $\text{mg L}^{-1}$ . These investigators also found a strong positive correlation between photosynthetic oxygen evolution rates in the photobioreactor cultures and the incident light intensity (PAR), which is consistent with the observed daily variations in DO concentrations in the climate-simulation pond cultures subjected to fluctuating incident light intensities and declining average light intensity over the duration of the experiment.

The areal biomass productivities (11.6 to 19.9  $\text{g m}^{-2} \text{day}^{-1}$ ) observed in this study are comparable to those reported for *Chlorella* sp. cultivated in other outdoor pond and photobioreactor systems (Table 1). In general, areal biomass productivities were positively correlated with culture temperature, with the highest productivity of 38.2  $\text{g m}^{-2} \text{day}^{-1}$  being observed in an open outdoor thin-layer photobioreactor where the daytime culture temperature was close to the optimum growth temperature of *Chlorella* sp. (ca. 36 °C) (Doucha and Livansky 2009). Even higher areal biomass productivities were measured for *C. sorokiniana* in indoor thin panel photobioreactors constantly maintained at the optimum growth temperature (37–38 °C) and continuously illuminated with high intensity LED lighting, i.e., 185  $\text{g m}^{-2} \text{day}^{-1}$  at 2100  $\mu\text{mol photons m}^{-2} \text{s}^{-1}$  and 94.1  $\text{g m}^{-2} \text{day}^{-1}$  at 800  $\mu\text{mol photons m}^{-2} \text{s}^{-1}$  (Cuaresma et al. 2009; Cuaresma-Franco et al. 2012). While these indoor cultivation studies provide an upper estimate of the optimum attainable biomass productivity of *C. sorokiniana* under different constant light and temperature conditions, these exceptional productivities are likely not achievable in outdoor cultivation systems subjected to diurnal temperature fluctuations and light-dark cycles, significant biomass losses due to dark respiration overnight and potential photo-inhibition during periods of high light intensity and low culture temperature (Jensen and Knutsen 1993; Vonshak et al. 2001; Edmundson and Huesemann 2015; Huesemann et al. 2016).

The photosynthetic efficiencies in the three climate-simulated pond culturing experiments ranged from 4.1 to 5.1%, which is close to PE values reported for most other outdoor *Chlorella* cultivation studies (Table 1). It appears that for the data shown in Table 1, there is a weak ( $R^2 = 0.49$ ) positive correlation between photosynthetic efficiency and cultivation temperature (Fig. 6). The highest and second highest PE values of ca. 14 and 11.7% were reported for studies where the cultivation temperature was always kept in the optimum

range (37–38 °C) and continuous illumination was supplied at 800 and 2100  $\mu\text{mol photons m}^{-2} \text{s}^{-1}$ , respectively (Cuaresma et al. 2009; Cuaresma-Franco et al. 2012). Clearly, cultivation at the optimum growth temperature, avoidance of biomass loss due to dark respiration overnight, and minimization of photo-inhibition commonly observed at high irradiances will result in high photosynthetic efficiencies that are unlikely to be achievable in outdoor ponds. Nevertheless, even in these optimized studies, the observed PE values were still significantly smaller than the theoretical optimum of 21% or 1.8  $\text{g mol}^{-1} \text{photons}$  (Cuaresma et al. 2009). Finally, the PE values shown in Table 1 for *Chlorella* spp. are in the same range as the PE values reported for outdoor cultivation studies involving other microalgal species, i.e., 3.8 to 14% (Bechet et al. 2013).

**Acknowledgements** This research was funded by the Bioenergy Technologies Office, US Department of Energy (Agreements DE-EE0006316 and DE-EE0006317), via subcontracts from New Mexico State University and California Polytechnic State University, San Luis Obispo, respectively. Additional support by the Department of Energy Science Undergraduate Laboratory Internship Program was provided to David Rye and Samuel Hobbs.

## References

- Batterton JC, Baalen CV (1971) Growth response of blue-green algae to sodium chloride concentration. Arch Microbiol 76:151–165
- Bechet Q, Munoz R, Shilton A, Guieysse B (2013) Outdoor cultivation of temperature-tolerant *Chlorella sorokiniana* in a column photobioreactor under low power-input. Biotechnol Bioeng 110: 118–126
- Convalves AMM, de Figueiredo DR, Pereira MJ (2005) The effects of different salinity concentrations on growth of three freshwater green algae. Fresenius Environ Bull 15:1382–1386
- Cuaresma M, Janssen M, Vilchez C, Wijffels RH (2009) Productivity of *Chlorella sorokiniana* in a short light-path (SLP) panel photobioreactor under high irradiance. Biotechnol Bioeng 104: 352–359
- Cuaresma-Franco M, Buffing MF, Janssen M, Vilchez Lobato C, Wijffels RH (2012) Performance of *Chlorella sorokiniana* under simulated extreme winter conditions. J Appl Phycol 24:693–699
- Doucha J, Livansky K (2006) Productivity,  $\text{CO}_2/\text{O}_2$  exchange and hydraulics in outdoor open high density microalgal (*Chlorella* sp.) photobioreactors operated in a middle and southern European climate. J Appl Phycol 18:811–826
- Doucha J, Livansky K (2009) Outdoor open thin-layer microalgal photobioreactor: potential productivity. J Appl Phycol 21:111–117
- Edmundson SJ, Huesemann MH (2015) The dark side of algae cultivation: characterizing night biomass loss in three photosynthetic algae, *Chlorella sorokiniana*, *Nannochloropsis salina*, and *Picochlorum* sp. Algal Res 12:470–476
- Fabregas J, Abalde J, Herrero C, Cabezas BV, Veiga M (1984) Growth of the marine microalga *Tetraselmis suecica* in batch cultures with different salinities and nutrient concentrations. Aquaculture 42: 207–215
- Goldman JC, Azov Y, Riley CB, Dennett MR (1982) The effect of pH in intensive microalgal cultures. I. Biomass regulation. J Exp Mar Biol Ecol 57:1–13
- Hase R, Oikawa H, Sasa C, Morita M, Watanabe Y (2000) Photosynthetic production of microalgal biomass in a raceway

- system under greenhouse conditions in Sendai City. *J Biosci Bioeng* 89:157–163
- Huesemann MH, Van Wagenen J, Miller T et al (2013) A screening model to predict microalgae biomass growth in photobioreactors and ponds. *Biotechnol Bioeng* 111:1583–1594
- Huesemann MH, Crowe B, Waller P, Chavis A, Hobbs S, Edmundson S, Wigmosta M (2016) A validated model to predict microalgae growth in outdoor pond cultures subjected to fluctuating light intensities and water temperatures. *Algal Res* 13:195–206
- Huesemann M, Dale T, Chavis A, Crowe B, Twary S, Barry A, Valentine D, Yoshida R, Wigmosta M, Cullinan V (2017) Simulation of outdoor pond cultures using indoor LED-lighted and temperature-controlled raceway ponds and Phenometrics™ photobioreactors. *Algal Res* 21:178–190
- Jensen S, Knutsen G (1993) Influence of light and temperature on photoinhibition of photosynthesis in *Spirulina platensis*. *J Appl Phycol* 5:495–504
- Kaewkannetra P, Enmak P, Chiu TY (2012) The effect of CO<sub>2</sub> and salinity on the cultivation of *Scenedesmus obliquus* for biodiesel production. *Biotechnol Bioprocess Eng* 17:591–597
- Kotrbaček V, Doubek J, Doucha J (2015) The chlorococcalean alga *Chlorella* in animal nutrition: a review. *J Appl Phycol* 27:2173–2180
- Lammers PJ, Huesemann M, Boeing W, Anderson DB, Arnold RG, Bai X, Bhole M, Brhanavan Y, Brown L, Brown J, Brown JK, Chisholm S, Meghan Downes C, Fulbright S, Ge Y, Holladay JE, Ketheesan B, Khopkar A, Koushik A, Laur P, Marrone BL, Mott JB, Nirmalakhandan N, Ogden KL, Parsons RL, Polle J, Ryan RD, Samocha T, Sayre RT, Seger M, Selvaratnam T, Sui R, Thomasson A, Unc A, Van Voorhies W, Waller P, Yao Y, Olivares JA (2017) Review of the cultivation program within the National Alliance for Advanced Biofuels and Bioproducts. *Algal Res* 22:166–186
- Lucker BF, Hall CC, Zegarac R, Kramer DM (2014) The environmental photobioreactor (ePBR): an algal culturing platform for simulating dynamic natural environments. *Algal Res* 6:242–249
- Moheimani NR (2013) Inorganic carbon and pH effect on growth and lipid productivity of *Tetraselmis sueica* and *Chlorella* sp. (Chlorophyta) grown outdoors in bag photobioreactors. *J Appl Phycol* 25:387–398
- Morita M, Wanatabe Y, Saiki H (2000) High photosynthetic productivity of green microalga *Chlorella sorokiniana*. *Appl Biochem Biotechnol* 87:203–218
- Neofotis P, Huang A, Sury K, Chang W, Joseph F, Gabr A, Twary S, Qiu W, Holguine O, Polle JEW (2016) Characterization and classification of highly productive microalgae strains discovered for biofuel and bioproduct generation. *Algal Res* 15:164–178
- Perkins W A, Richmond MC (2004) MASS2, Modular Aquatic Simulation System in Two Dimensions: theory and numerical methods. Report PNNL-14820-1, Pacific Northwest National Laboratory, Richland, Washington
- Rachlin JW, Grosso A (1991) The effects of pH on the growth of *Chlorella vulgaris* and its interactions with cadmium toxicity. *Arch Environ Contam Toxicol* 20:505–508
- Renaud S, Parry D (1994) Microalgae for use in tropical aquaculture II: effect of salinity on growth, gross chemical composition and fatty acid composition of three species of marine microalgae. *J Appl Phycol* 6:347–356
- Sogaard DH, Hansen PJ, Rysgaard S, Glud RN (2011) Growth limitation of three Arctic Sea ice algae species: effects of salinity, pH, and inorganic carbon availability. *Polar Biol* 34:1157–1165
- Sorokin C (1959) Tabular comparative data for the low- and high-temperature strains of *Chlorella*. *Nature* 185:613–614
- Spolaore P, Joannis-Cassan C, Duran E, Isambert A (2006) Commercial applications of microalgae. *J Biosci Bioeng* 101:87–96
- Unkefer CJ, Sayre RT, Magnuson JK, Anderson DB, Baxter I, Blaby IK, Brown JK, Carleton M, Cattolico RA, Dale T, Devarenne TP, Downes CM, Dutcher SK, Fox DT, Goodenough U, Jaworski J, Holladay JE, Kramer DM, Koppisch AT, Lipton MS, Marrone BL, McCormick M, Molnár I, Mott JB, Ogden KL, Panisko EA, Pellegrini M, Polle J, Richardson JW, Sabarsky M, Starkenburg SR, Stormo GD, Teshima M, Twary SN, Unkefer PJ, Yuan JS, Olivares JA (2017) Review of the algal biology program within the National Alliance for Advanced Biofuels and Bioproducts. *Algal Res* 22:187–215
- US Department of Energy (DOE), Office of Energy Efficiency and Renewable Energy (2016) Bioenergy Technology Office—Multi-year program plan, page A-2. <https://www.energy.gov/eere/bioenergy/downloads/bioenergy-technologies-office-multi-year-program-plan-march-2016>
- US Department of Energy (DOE), Office of Energy Efficiency and Renewable Energy, Biomass Program (2010) National algal biofuels technology roadmap. <https://doi.org/10.2172/1218560>. <https://energy.gov/eere/bioenergy/downloads/national-algal-biofuels-technology-roadmap>
- Van Auken OW, McNulty IB (1973) The effect of environmental factors on the growth of a halophilic species of algae. *Biol Bull* 145:210–222
- Van Wagenen J, Miller TW, Hobbs S, Hook P, Crowe B, Huesemann MH (2012) Effects of light intensity and temperature on fatty acid composition in *Nannochloropsis salina*. *Energies* 5:731–740
- Vonshak A, Torzillo G, Masojidek J, Boussiba S (2001) Sub-optimal morning temperature induces photoinhibition in dense outdoor cultures of the alga *Monodus subterraneus* (Eustigmatophyta). *Plant Cell Environ* 24:1113–1118
- Wigmosta MS, Coleman AM, Skaggs RJ, Huesemann MH, Lane LJ (2011) National microalgae biofuels production potential and resource demand. *Water Resour Res* 47(3). <https://doi.org/10.1029/2010WR009966>
- Williams PJB, Laurens LML (2010) Microalgae as biodiesel & biomass feedstocks: review & analysis of the biochemistry, energetics, & economics. *Energy Environ Sci* 3:554–590
- Yandu L, Chi X, Li Z, Yang Q, Li F, Liu S, Gan Q, Qin S (2010) Isolation and characterization of a stress-dependent plastidial D12 fatty acid desaturase from the Antarctic microalga *Chlorella vulgaris* NJ-7. *Lipids* 45:179–187